4417

3D High-Resolution Reduced Field-of-View T2-Weighted Imaging by Combining 3D EPI and Spatially Selective Pulses

Jiayao Yang[1], Jon-Fredrik Nielsen[1,2,3], Jeffrey A. Fessler[1,2,3], and Yun Jiang[2,3]
[1]Department of Electrical Engineering and Computer Science, University of Michigan, Ann Arbor, MI, United States, [2]Department of Biomedical Engineering, University of Michigan, Ann Arbor, MI, United States, [3]Department of Radiology, University of Michigan, Ann Arbor, MI, United States

Synopsis

Keywords: RF Pulse Design & Fields, RF Pulse Design & Fields, reduced FOV, 3D EPI

Motivation: Multidimensional selective RF pulses combined with nonselective pulses has been studied in achieving reduced FOV (rFOV) imaging. However, combining of multiple spatial selective pulses may improve the spatial selectivity and help achieve 3D high-resolution rFOV imaging at 3T.

Goal(s): To achieve high-resolution 3D rFOV T2-weighted images by using multidimensional RF pulses.

Approach: Combining two 3D selective RF pulses respectively for excitation and refocusing, and a 3D EPI imaging sequence at a 3T scanner.

Results: High-resolution 3D images of brain and prostate were acquired using proposed method.

Impact: Our simulation and in vivo results demonstrated the potential of obtained high-resolution T2-weighted images in the brain and prostate. This shows the potential to achieve high-resolution diffusion imaging using rFOV imaging approach in the future study.

Introduction

Reduced Field-of-View (rFOV) imaging, achieved by applying multidimensional spatially selective pulses, can increase sampling efficiency and reduce artifacts from outside region-of-interest (ROI). However, the quality of rFOV images is heavily dependent on the spatial selectivity provided by these RF pulses. Designing multidimensional pulses, especially in 3D, is challenging and result in poor excitation profiles, long pulse duration[1-3], or extended calculation times[4-5], which have hindered the practical implementation of rFOV imaging.

The goal of this study is to demonstrate the feasibility of achieving high-resolution 3D rFOV imaging using two 3D spatially selective RF pulses. We designed 3D RF pulses for excitation (90°) and refocusing (180°) using an efficient auto-differentiable algorithm[6] based on the spin-domain representation[7]. Our designed pulses have a pulse duration of 4.15 ms, comparable to 1D pulses, allowing them to be effectively incorporated into spin-echo type sequences. We demonstrated that the combination of two 3D RF pulses improved spatial selectivity through simulations and in vivo experiments performed on the brain and prostate.

Methods

RF pulse design: The algorithm is based on the spin-domain based RF pulse optimization method[8]. We formulated the design problems for excitation and refocusing as:

$$\arg\min_{\mathbf{b},\mathbf{g}} \square = \sum_{i=1}^{N} w_i \left\{ |\alpha^*_{T,i}(\mathbf{b},\mathbf{g})\beta_{T,i}(\mathbf{b},\mathbf{g}) - \frac{1}{2}e^{i\phi}\sin\theta_i|^2 + (|\beta_{T,i}(\mathbf{b},\mathbf{g})| - |\beta_{D,i}|)^2 \right\} + \lambda\|\mathbf{b}\|_2^2, \quad \text{subject to} \quad \text{hardware}\sim\text{limits}$$

$$\arg\min_{\mathbf{b},\mathbf{g}} \square = \sum_{i=1}^{N} w_i |\beta^2_{T,i}(\mathbf{b},\mathbf{g}) - \beta^2_{D,i}| + \lambda\|\mathbf{b}\|_2^2, \quad \text{subject to} \quad \text{hardware limits}$$

where $\mathbf{b}$ is the RF waveform, $\mathbf{g}$ is the gradient waveform, α_T and β_T are the spin-domain representation[9] of the magnetization behaviors, α_D and β_D are desired targets, w_i is the weighting function for different spins, N is the total number of spins, ϕ is the phase of the excitation, and is the regularization parameter to constrain the RF energy. We solved the design problems considering hardware limitations such as peak RF of 14 uT, maximum gradient of 24 mT/m, and maximum slew-rate of 120 mT/m/ms.

Pulse Sequence: A spin-echo sequence with 3D EPI acquisition (as shown in Figure 1) was implemented using [10] All experiments were performed at 3T (Vida, Siemens Healthineers) with a matrix size of 128×128×32, TR=1s, TE=64ms. EPI had 75% partial Fourier with an acceleration factor of 2. The scan time for one average was 32 seconds.

Phantom experiments: 3D pulses were designed to excite an ROI of 8×8×6 cm^3. The performance of combining two 3D RF pulses (3D 90 + 3D 180) were evaluated by simulation and examined in a phantom experiment by comparing the results acquired using sequences with 1) 1D 90 + 1D 180; 2) 3D 90 + 1D 180; 3) 1D 90 + 3D 180 with an FOV of 300×300×96mm^3.

In vivo experiments: The study was approved by the Institutional Review Board and informed written consent was obtained from each participant. Brain and prostate imaging were performed in 4 participants. 3D pulses were designed with ROI sizes of 6×6×6 cm^3 for the brain and of 9×9×6 cm^3 for the prostate, respectively. The scan time was 32 seconds in the brain with 1 average and 64 seconds with 2 averages in the prostate. The spatial selectivity was evaluated by dividing outer volume signal by signal within ROI. Full FOV and rFOV images were acquired as same as the phantom experiments.

Results

Figure 1 shows the sequence diagram and RF and gradient waveforms of designed 3D excitation and refocusing pulses.
Figure 2 shows the simulation results of the designed 3D excitation and refocusing pulse, and their combined performance. The combination of 3D excitation and 3D refocusing had smallest signal error which suggested that combining two pulses lead to better spatial selectivity.
Figure 3 shows the 3D SE phantom images and their 1D signal profiles using different combinations of RF pulses. The combination of 3D excitation and 3D refocusing pulses showed best suppression of outer volume signals.
Figure 4 and Figure 5 respectively show the 3D SE images of the brain and prostate. The images acquired using 3D 90 + 3D 180 pulses in both the brain and prostate had the lowest relative outer volume signals. Higher spatial resolution (1×1×3 mm^3) 3D images of both the brain and prostate were acquired using the rFOV method without aliasing. rFOV prostate EPI images showed less distortion than full FOV images compared with TSE images.

Conclusions and Discussion

In this study, we explored the application of 3D excitation and 3D refocusing pulses designed using spin-domain based optimization in the acquisition of high-resolution 3D rFOV imaging methods. We successfully acquired high-resolution 3D images in the brain and prostate and demonstrated better suppression of outer volume signals using multiple 3D selective pulses. In the future, this will be explored in achieving high-resolution diffusion-weighted rFOV images.

Acknowledgements

This study was supported by NIH grants R37CA263583, R01CA284172, and R01EB032378, and Siemens Healthineers.

References

1. Rieseberg, Susanne, Jens Frahm, and Jurgen Finsterbusch. "Two-dimensional spatially-selective RF excitation pulses in echo-planar imaging." Magnetic Resonance in Medicine: An Official Journal of the International Society for Magnetic Resonance in Medicine 47.6 (2002): 1186-1193.
2. Saritas, Emine Ulku, et al. "DWI of the spinal cord with reduced FOV single-shot EPI." Magnetic Resonance in Medicine: An Official Journal of the International Society for Magnetic Resonance in Medicine 60.2 (2008): 468-473.
3. Mitsouras, Dimitris, Robert V. Mulkern, and Frank J. Rybicki. "Strategies for inner volume 3D fast spin echo magnetic resonance imaging using nonselective refocusing radio frequency pulses a." Medical physics 33.1 (2006): 173-186.
4. Luo, Tianrui, et al. "Joint design of RF and gradient waveforms via auto-differentiation for 3D tailored excitation in MRI." IEEE transactions on medical imaging 40.12 (2021): 3305-3314.
5. Setsompop, Kawin, et al. "Magnitude least squares optimization for parallel radio frequency excitation design demonstrated at 7 Tesla with eight channels." Magnetic Resonance in Medicine: An Official Journal of the International Society for Magnetic Resonance in Medicine 59.4 (2008): 908-915.
6. Malik, Shaihan J., and Joseph V. Hajnal. "3D-FSE inner volume imaging using 3D selective excitation." Proc. Intl. Soc. Magn. Reson. Med. Vol. 948. 2014.
7. Sun, Kaibao, et al. "Three-dimensional reduced field-of-view imaging (3D-rFOVI)." Magnetic resonance in medicine 87.5 (2022): 2372-2379.
8. Yang, Jiayao, et al. "Multidimensional RF pulse design in spin-domain using auto-differentiation for 3D refocusing pulse.", 2023 ISMRM Annual Meeting, Toronto, ON, Canada
9. Pauly, John, et al. "Parameter relations for the Shinnar-Le Roux selective excitation pulse design algorithm (NMR imaging)." IEEE transactions on medical imaging 10.1 (1991): 53-65.
10. Layton, Kelvin J., et al. "Pulseq: a rapid and hardware-independent pulse sequence prototyping framework." Magnetic resonance in medicine 77.4 (2017): 1544-1552

Figures

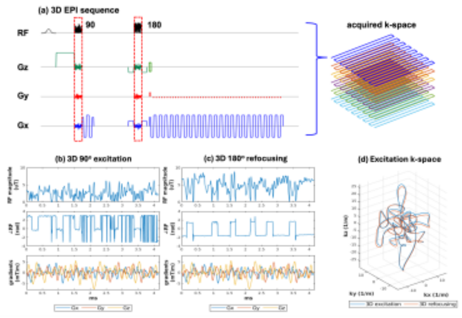

(a) Sequence used in the study of which the 90^{o} excitation and 180^{o} refocusing pulses were replaced by 3D selective excitation and refocusing RF pulses and illustration of acquired 3D k-space. (b) Designed 3D 90^{o} excitation pulse. (c) Designed 3D 180^{o} refocusing pulses. (d) Excitation k-space trajectory of gradient waveforms of designed 3D excitation and 3D refocusing pulses.

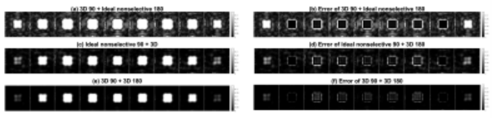

(a)(b) Simulated signal and error of 3D excitation pulse + ideal nonselective refocusing pulse at different slice positions (9 slices position of FOV=300×300×96 mm^3 are displayed). (c)(d) Simulated signal and error of ideal nonselective excitation + 3D refocusing pulse at the same slice positions. (e)(f) Simulated signal and error of 3D excitation + 3D refocusing. The MSE of simulated signal and desired signal: (b) is 0.0131; (d) is 0.0024; (f) is 0.0008. Combining 3D excitation and 3D refocusing pulses produces the lowest outer volume magnetization.

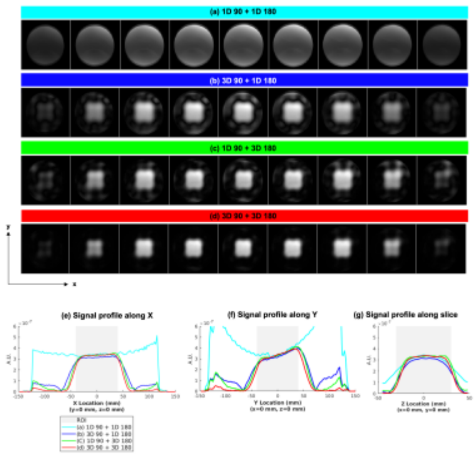

(a-d) 3D SE images of phantom acquired using different RF pulses: 1D 90 + 1D 180; 2D 90 + 1D 180; 1D 90 + 3D 180; 3D 90 + 3D 180. (e-g) 1D profile of the acquired signal intensity along x, y, and z directions. The 3D 90 + 3D 180 has the lowest outer volume signal intensity.

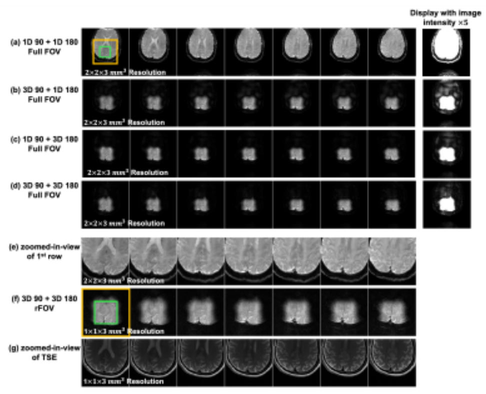

(a-d) 3D brain SE images acquired using stack-of-EPI and different RF pulses. The full FOV is 256×256×96 mm^3 and ROI is 6×6×6 cm^3 (green), and the spatial resolution is 2×2×3 mm^3. The relative outside ROI signal intensities are: (a) 0.1789; (b) 0.0380; (c) 0.0249; (d) 0.0245. The 3D 90 + 3D 180 has the lowest relative outer volume signal intensity. (e) Zoomed in view (rFOV) of 1D 90 + 1D 180 results. The rFOV is indicated as the orange box in full FOV image. (f) rFOV 3D brain images. The spatial resolution is 1×1×3 mm^3. (g) Zoomed in view (rFOV) of reference TSE images (TE=62 ms).

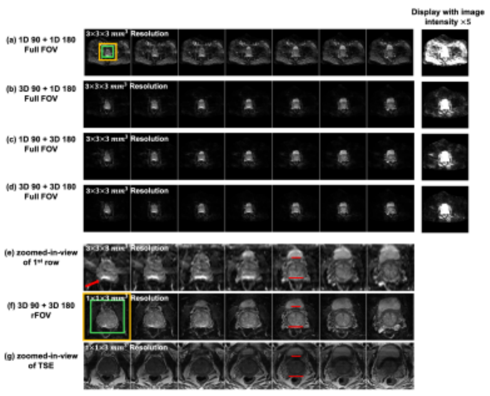

(a-d) 3D prostate SE images acquired using stack-of-EPI and different RF pulses, full FOV 384x384x96 mm^3, ROI 9x9x6 cm^3 (green), spatial resolution 3x3x3 mm^3. The relative outer volume signal intensities: (a) 0.2321; (b) 0.0896; (c) 0.0677; (d) 0.0579. The 3D 90 + 3D 180 has the lowest relative outer volume signal. (e) Zoomed in view (rFOV, 128x128x96 mm^3, orange) of 1D 90 + 1D 180 results. (f) rFOV 3D prostate images, spatial resolution 1x1x3 mm^3. (g) Zoomed in view (rFOV) of TSE images (TE=62 ms). rFOV images (f) shows less distortion than (e) compared with TSE (marked by a pair of red bars).

Proc. Intl. Soc. Mag. Reson. Med. 33 (2025)
4417